
Article:
Aravind, B., Khandelwal, B. orcid.org/0000-0001-9295-188X and Kumar, S. (2018) Experimental investigations on a new high intensity dual microcombustor based thermoelectric micropower generator. Applied Energy, 228. pp. 1173-1181. ISSN 0306-2619

https://doi.org/10.1016/j.apenergy.2018.07.022

Experimental investigations on a new high intensity dual microcombustor based thermoelectric micropower generator

B. Aravind[1,*], Bhupendra Khandelwal[2], Sudarshan Kumar[1].

[1]Department of Aerospace Engineering, Indian Institute of Technology Bombay, Powai, Mumbai 400076, India

[2]Low Carbon Combustion Centre, University of Sheffield, Unit 2, Crown Works Industrial Estate, Rotherham Road, Sheffield S20 1AH, United Kingdom

Abstract

A new concept of dual microcombustor based thermoelectric micropower generator with high power density (~0.14 mW/mm^3) and high conversion efficiency (4.66 %) is reported in this work. A new configuration with a dual microcombustor system is experimentally investigated with two thermoelectric modules and operates with liquefied petroleum gas as fuel. The dual microcombustor is fabricated using a rectangular aluminium metal block and detailed investigations on flame stability limits and thermal characteristics were carried out. Dual microcombustor configuration helps to significantly improve the flame stability limits and thermal characteristics over the single combustor configuration due to increased flame-surface interaction and enhanced heat recirculation through solid walls. Maximum power point tracking (MPPT) algorithm is applied to achieve a maximum power output of 4.52 W with a maximum conversion efficiency of 4.66 %. The application of porous media significantly helped improve the upper flame stability limits with a maximum conversion efficiency of 4.32 %, and 4.66 %, at ϕ = 1 and 0.9 respectively at 10 m/s mixture velocity. The system compactness and high output power with significantly improved conversion efficiency shows the possibility of its application in various portable micro-scale power generators for remote, stand-alone, military and aerospace applications.

Keywords: Microcombustor, Thermoelectric generator, Flame stability, Conversion efficiency, Porous media

Nomenclature

I – Current (A)

m^* – Inlet mixture flow rate (kg/s)

P_{in} – Input power (W)

P_{aux} – Pumping power (W)

P_{out} – Electrical power output (W)

Q_s – Heat supplied to module (W)

Q_r – Heat rejected from module (W)

R_i – Internal resistance of module (Ω)

R_L – Load resistance (Ω)

t_p – Porous media thickness (m)

T_{Cold} – Cold side temperature (K)

T_{Hot} – Hot side temperature (K)

$T_{surface}$ – Average surface temperature (K)

U_{in} – Inlet mixture velocity (m/s)

V^*_w – Volume flow rate of coolant (lpm)

Greek symbols

ϕ - Equivalence ratio

Ω - Unit of electric resistance

η_{con} – Conversion efficiency

Abbreviations

LFSL- Lower flame stability limit

MPPT – Maximum power point tracking

TEG – Thermoelectric generator

UFSL- Upper flame stability limit

1 Introduction

There is a strong motivation to develop combustion-based portable power systems in the past few decades due to fast development and implementation of micro electromechanical systems (MEMS) in various platforms and small power requirement by these systems for their efficient operation. The usage of conventional electrochemical batteries as a power source is limited in various military, aerospace and standalone applications due to its inherent disadvantages such as long recharging time, heavy weight, low energy density and adverse environmental impacts [1]. Hydrocarbon fuel-based power source with a conversion efficiency of ~ 5 %, would result in six times higher power density than advanced electrochemical battery concepts as illustrated in Fig. 1a. Therefore, combustion-based systems for power generation are considered to be a viable alternative to conventional electrochemical batteries owing to their high-power density, light weight and compact size [2]. The power delivered by various conventional electrochemical batteries has a sloping discharge curve and it falls progressively throughout its discharge cycle as shown in Fig. 1b. This could give rise to various problems in the system performance, particularly those requiring a constant voltage supply throughout their operation. Therefore, the combustion-based micropower generators could provide a better alternative as they are capable of providing a constant power throughout the operational time with minimum recharge time as shown in Fig. 1b. The hydrocarbon fuels have 50 –100 times higher energy density than conventional electrochemical batteries [3]. Therefore, various innovative methods to use combustion-based power generators for such applications have been pursued by researchers all over the world [4, 5]. Flame stabilization in such small-scale combustors still continues to be a challenging task due to its increased surface to volume ratio [6]. The strong thermal-wall coupling together with the reduced residence time results in increased tendency of flame quenching through radical and thermal quenching routes [7]. Researchers have implemented various innovative techniques of excess enthalpy combustion [8-10] and catalytic combustion [11, 12] to resolve the flame quenching issues at such small scales. Chou et al. [10] studied the effect of porous media on micro combustor performance.

Their results show that higher and superior uniform temperature distribution along the combustor wall can be achieved with the application of porous media. Vijayan et al. [11] studied the importance of heat recirculation on meso scale combustor by performing a detailed parametric study on combustor performance by varying the combustor material, inlet conditions etc. Thorough investigations on various aspects of flame stabilization in swiss roll combustor by Shirsat and Gupta [13] and Wierzbicki et al. [14] indicate that extended extinction limits and combustion stability can be achieved with proper thermal management in the swiss roll combustors. This concept in the context of thrust generation for various applications such as small robotics and nanosatellites also explored by same research group using methanol as fuel [15]. Numerous numerical studies have been performed to understand the flame stabilization and its dynamics in microchannels in past decade [16-20]. Wan and Zhao [17] investigated the flame dynamics in a novel preheating micro combustor suitable for portable power applications. They observed a wide stability and various instability regimes due to the interplay between flame speed and flow velocity. Alipoor et al.[18] and Akhtar et al. [20] performed a numerical study on curved micro combustors suitable for photovoltaic power generation applications. The result shows a significant increase in the flame stability limits and combustor wall temperature for the curved micro combustor compared to the straight channel micro combustors. They observed a wide stability and various instability regimes due to the interplay between flame speed and flow velocity. Zuo et al. [21] used rectangular rib in the micro-cylindrical combustor for better flame stabilization. They conducted a detailed parametric study on the geometry of ribs to achieve maximum wall temperature and uniform temperature distribution. Since, the conventional chemical batteries are outperformed due to aforementioned issues, several combustion-based micropower generation systems such as micro gas turbine [22], micro thermophotovoltaic generators [23, 24], fuel cells [25] and thermoelectric generators [26-30], were recently proposed and investigated. Although, heat engines could be commonly proposed, their significant heat and friction losses due to the presence of moving parts make them impractical for various applications at such small scales because of strong noise and low conversion efficiencies. Thermoelectric and thermophotovoltaic power generators are simple systems

and subjected to less maintenance issues due to absence of moving parts [31, 32]. Cho et al. [33] have reviewed several micropower generation systems and provided deep insights into recent advancements of such systems.

Several efforts have been made by researchers on TPV [23, 24] and fuel cell [25] based micropower generators. Yang et al. [23] developed a micro thermophotovoltaic power generator using backward stepped combustor with 0.113 cm^3 volume. The system delivered 1.02 W power output with hydrogen fuel. A single chamber solid-oxide fuel cell (SOFC) integrated with a Swiss-roll combustor by Ahn et al. [25] was shown to achieve power densities of 420 mW/cm^2. They studied the extinction limits and thermal behaviour of the system and achieved efficient performance even at low Reynolds numbers. In comparison with the fuel cells and other combustion-based power systems, thermoelectric systems are promising due to their low energy consumption, compactness, system reliability and long life of modules. However, the low conversion efficiency of such systems is still an issue requiring attention of material researchers [34, 35].

A TE based power generator using Silicon-coated catalytic combustor fabricated by Yoshida et al. [26] was able to produce 184mW power with 2.8 % conversion efficiency. Shimokuri et al. [28] developed a mesoscale vortex combustor integrated with TE modules. Their result suggests that the heat transfer was significantly enhanced due to formation of vortex flow and produced a system efficiency of 3 % with a power output of 18.1 W. Yadav et al. [29] used a three-step combustor with a recirculation cup as a heating source. They reported that the overall conversion efficiency was improved from 1.2 % (single module) to 4.6 % for four-module configuration using the same combustor. Merotto et al. [30] coupled a catalytic combustor with a TEG (thermoelectric generator) and achieved a conversion efficiency of 2.85 % with a 9.86 W of electric power output. Recently, the same research group have developed a compact power source using the similar catalytic micro combustor capable of delivering power output up to 1 W [36].

In the present study, a new dual microcombustor configuration based micropower generator has been proposed and experimentally investigated. The flame stability limits, combustion and thermal characteristics are investigated in detail. Two TEG modules are installed with appropriate heat sinks to achieve maximum power output from the setup.

Although, several numerical studies [37, 38] have been reported in literature on multi-combustor configurations, an experimental demonstration of such configuration for portable power generation needs to be implemented and explored. The system compactness and output power with high conversion efficiency shows the possibility of its application in various portable scale power generators for remote, stand-alone, military and aerospace applications. The novelty of the present work lies in the configuration of the micro combustor and the performance of the micropower generator having higher power density (0.14 mW/mm^3) with higher conversion efficiency (4.66 %) .

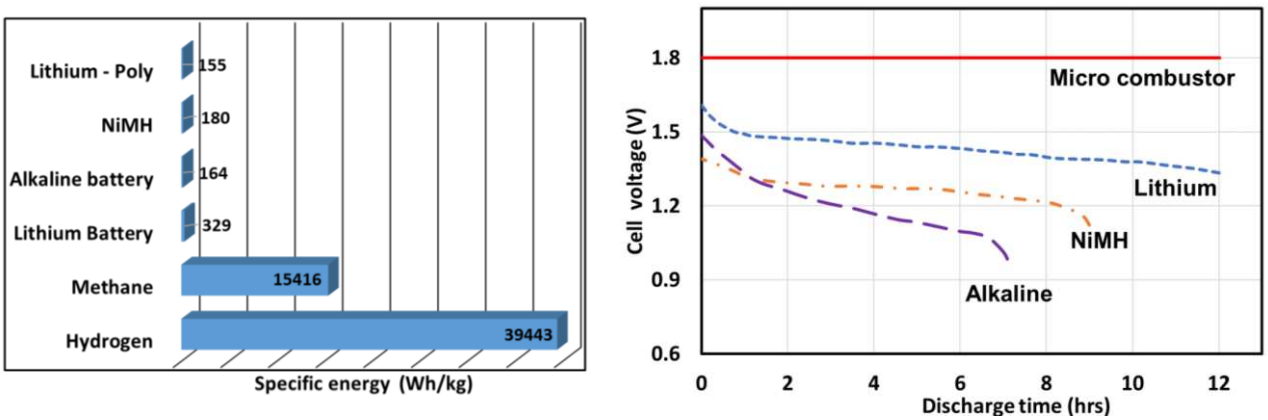

(a) (b)

Fig. 1 (a) Comparison of the energy density of hydrocarbon fuels with conventional electrochemical batteries. (b) Comparison of discharge curve of different battery systems and microcombustor based power generation system.

2 Experimental setup details

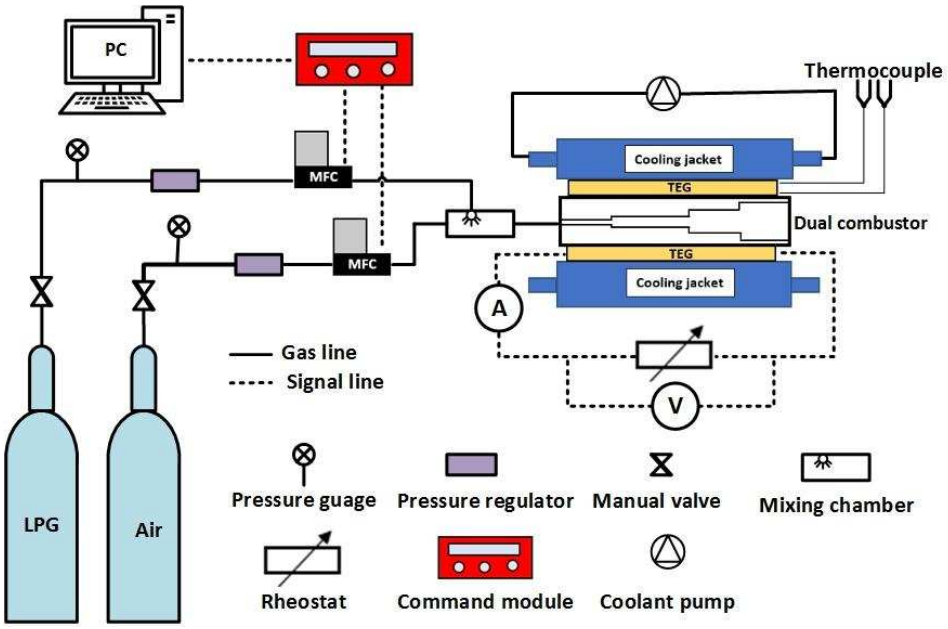

Fig. 2 Schematic of experimental setup.

Experimental setup consists of high pressure air, fuel tank, precision electric mass flow controllers (MFC), pipeline and integrated micro combustor-thermoelectric generator system with power measuring equipments as shown in Fig. 2. The required mass flow rates of LPG and air were supplied using two separate electronic mass flow controllers (0 – 0.5 lpm for LPG and 0 – 2.0 lpm for air) controlled through command module connected to a computer. The fuel and air are thoroughly mixed in the mixture chamber prior to the micro combustor inlet. The fuel is injected as a high velocity stream into the fresh air in the mixing chamber to ensure complete mixing. Fuel-air mixture is ignited using a pilot flame from a butane torch at the ignition port. The ignition port is closed after the flame established in the combustion chamber to ensure exhaust gas recirculation through the microcombustor. The accuracy of the measured mass flow rates is ± 1 % of the full scale. In order to measure the temperature on the outer walls of the heating medium, K type thermocouples of 0.5 mm bead diameter with an accuracy of ± 2 % were used.

The dimensional details of the micro combustor are depicted in Fig. 3a. The dual microcombustor with backward steps and two recirculation holes is fabricated inside a rectangular aluminium metal block

of size 32×32×10 mm^3. The dimensions of the heating medium are chosen to ensure their matching with the dimensions of the thermoelectric modules. Aluminium is chosen owing to it high thermal conductivity and lightweight.

2.1 Details of microcombustor and the micropower generator

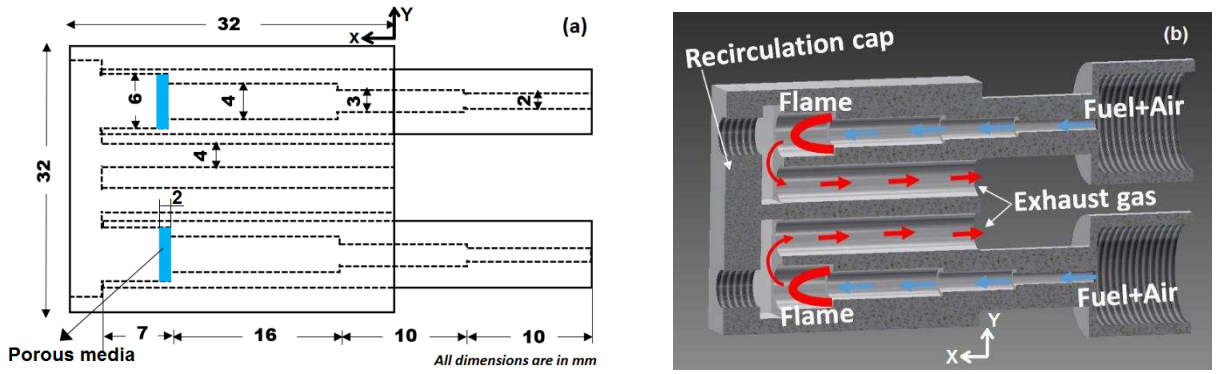

Fig. 3 (a) Dimensional details (b) Cross-section view of the dual microcombustor configuration.

The mixture inlet diameter of the microcombustor is 2 mm, which gradually increases to 6 mm in steps as shown in Fig. 3 a and b. Total mixture velocity (U_{in}) is calculated based on the inlet area corresponding to 2 mm diameter. The total mixture is equally divided into two combustors through the two 2 mm inlets of the dual combustor. The combustor dimensions are same to author's previous studies [29, 39]. The steps provided in the micro-combustor create a sudden flow expansion, which induces local recirculation near the steps. This helps increase the local residence time of fuel-air mixture and enhances the flame stability limits [40-42]. In addition to these micro-combustors, two 4 mm diameter holes are provided to dispel the combustion products. These holes further help to extract excess enthalpy from exhaust gases and preheat the fresh incoming mixture and simultaneously transfer excess heat to thermoelectric modules. Detailed investigations have been carried out to understand the effect of heat recirculation on flame stability limits and power generation as discussed in the following sections.

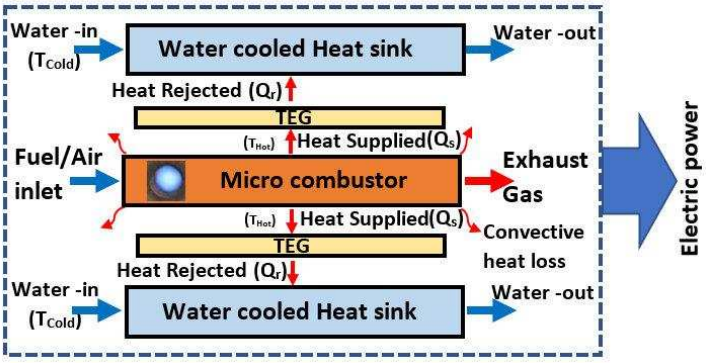

Fig. 4 Conceptual diagram of thermoelectric power generator.

The basic working principle of a thermoelectric power generator is illustrated in Fig. 4. A heat source or micro combustor, a heat sink and a thermoelectric generator (TEG) are the three essential parts of any micro thermoelectric power generator. A temperature gradient is created across the TEG by a heat source and heat sink in turn induces the electron flow through Seebeck effect. An actual photograph of the dual and single [39] microcombustor with thermoelectric modules is shown in Fig. 5 a and b respectively. The system consists of two commercially available Bi_2Te_3 thermoelectric modules (TEG) sized 30×30×3 mm^3 from Nippon India Ltd. mounted on top and bottom side of the microcombustor along with multi-pass cooling jackets [39]. These thermoelectric modules consist of number of semiconductor couples connected thermally in parallel and electrically in series connections. The semiconductor legs of these modules are mounted between two 0.8 mm thick ceramic wafers to provide electrical insulation. This module has a capacity of delivering a maximum power of 4.6 W for a temperature difference of 220 K. A continuous film of thermal paste was applied on the either side of the TEG to enhance the heat transfer. All the measuring equipments are calibrated before commencing the experiment. The total uncertainty in the reported data is less than ± 1.5 % for all experiments reported in this work [39].

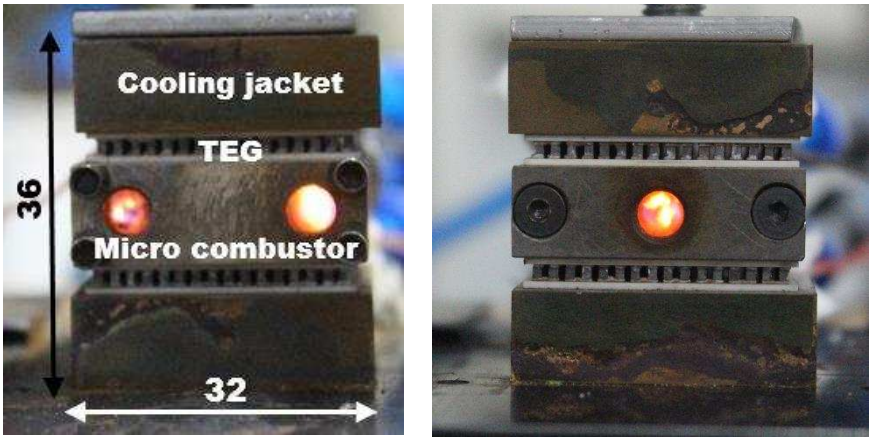

(a) (b)

Fig. 5 Actual photograph of stabilized in a (a) Dual combustor (b) single combustor power generator.

3 Results and discussion

3.1 Combustion characteristics without TEGs

Initially, detailed experiments are carried out to evaluate the thermal performance of the new dual microcombustor configuration before adopting it for power generation using thermoelectric modules. Flame stability limits and thermal characteristics are investigated as discussed below.

3.1.1 Effect of porous media on flame stability limits

Ceramic fibre wool, used as the porous medium in the present study, has a porosity of 0.92, density of 2600 kg/m^3, specific heat of 850 kJ/kg K, thermal conductivity of 0.03 W/m K and emissivity of 0.8. Porous media helps to store the heat and preheat the incoming mixture and in turn increases the flame speed through heat recirculation. A porous media is placed at the third step as shown in Fig. 3a to enhance the flame stability limits. The effect of the thickness of porous media (t_p) is investigated to decide the optimum thickness as shown in Fig. 6a. It is clear that almost same surface temperature ($T_{surface}$) is observed for t_p = 0 and 2 mm and it reduces with an increase in porous media thickness. The flame is observed to quench at t_p = 4 mm, 7 mm and 10 mm for 3 m/s, 5 m/s and 7 m/s velocity

respectively due to a significant reduction in the flow velocity and poor preheating of the incoming mixture. Therefore porous media of 2 mm thickness has been used in the present study. A self-sustained flame is observed at different steps of the micro-combustor based on the operating conditions[40, 41]. A conical flame is formed which anchors at different steps and its position changes with an increase in mixture velocity at a fixed equivalence ratio. A flame stability diagram is plotted to understand the operating regime of the micro-combustor configuration. The terms upper flame stability limit (UFSL) and lower flame stability limit (LFSL) are used to defined the maximum and minimum mixture velocity at which a sustained flame is achieved in the combustor for a fixed equivalence ratio to understand the operating regime of the micro combustor. Fig. 6b shows the flame stability regime of the proposed dual combustor with and without porous media at the third step, keeping the ignition port open (no heat recirculation). A stable flame is observed for a minimum thermal input of ~ 10 W. Upper flame stability limit is not observed with heat recirculation case (closed ignition port condition) for both (porous and non-porous) the conditions. However, flame extinction occurs at intermediate fuel flow rate conditions for free flame condition (non-porous media), when the combustor is integrated with module and cooling jacket, due to excessive heat transfer. Therefore, to further improve the microcombustor performance, a ceramic wool based porous media of 2 mm thickness was inserted at the third step of the dual microcombustor. The ceramic wool significantly helped to sustain the flame at higher flow rates and helped increase the heat recirculation [43]. The lower flame stability limit (LFSL) remained nearly same to that of free flame case. No upper flame stability limit (UFSL) was observed with the porous media, even when the modules were mounted on the combustor as shown in Fig. 6b.

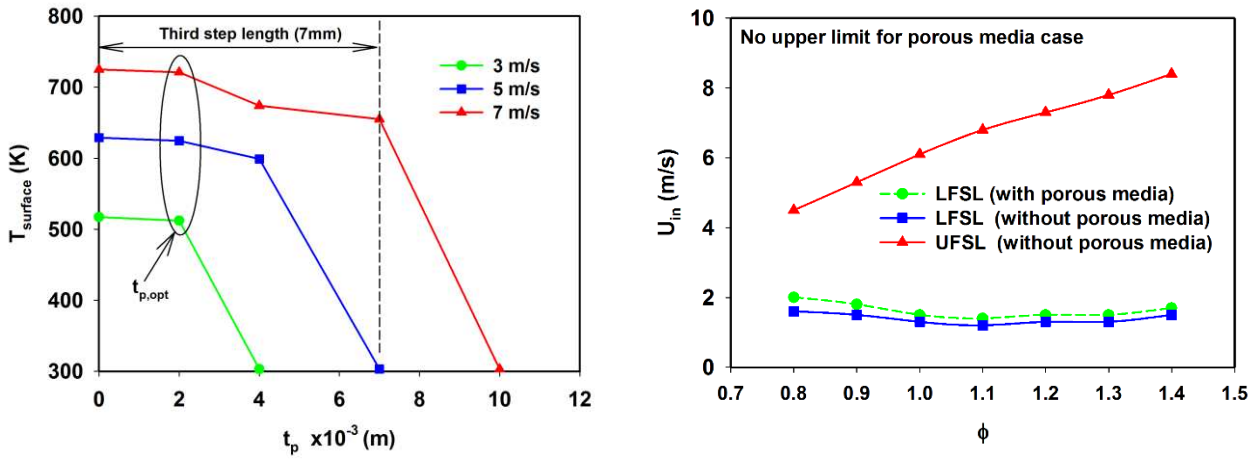

(a) (b)

Fig. 6 (a) Effect of porous media thickness on thermal characteristics. (b) Effect of porous media on flame stability regime of dual microcombustor.

The composition of the LPG as provided by the supplier is 60 % butane and 40 % propane. Fuel flow rate multiplied with its calorific value helps obtain the thermal input to the system. Combustion completeness is measured through detailed exhaust gas analysis using a gas chromatograph and flue gas analyzer. These studies on combustion completeness have been reported earlier by Deshpande et al. [44],Taywade et al. [41] and Fan et al.[45]. The combustion was nearly 98 – 99% complete.

3.1.2 Temperature distribution

Figure 7a and 7b show the wall temperature and temperature uniformity of the proposed dual microcombustor configuration, a pre-requisite characteristic for TEG based power generation system. Figure 7a shows the temperature distribution on the combustor surface for 6.0 m/s mixture velocity and $\phi = 1$. Even though, there is a monotonic increase in the surface temperature along the axial direction up to x = 19.2 mm, a slight overlap in peak temperature is observed between x = 25.6 and 32 mm locations. This variation is perhaps due to the flame location and a spread in the distribution of temperature is due to presence of porous media at 25.6 mm (third step) location. However, it is to be noted that the overall variation of surface temperature is less than 10 K along x and y-axis, which confirms to the requirement of temperature uniformity at the outer surface. Figure 7b shows the

comparison of average surface temperature and exhaust gas temperature for a single and dual microcombustor configurations at $\phi = 1.0$ with mixture velocities. The average temperature is obtained using equidistant points along the central line on outer surface of the combustor. It is observed that the average surface temperature reaches around 673 K for 6.0 m/s mixture velocity. However, this temperature drops significantly to safe operating limits of the modules (< 523 K), when the modules are mounted on the combustor even at higher mixture velocities.

There is a significant increase in heat transfer from exhaust gas to combustor wall for the dual combustor configuration as compared to single combustor [39] ($\Delta T_{dual} < \Delta T_{single}$) as clear from Fig. 7b. This is due to increased heat recirculation and increased flame-wall interaction. Overall, ~ 15 K rise is obtained for dual combustor configuration at the same flow rate conditions. The increased heat transfer in dual microcombustor configuration would help in improving the output power and overall conversion efficiency of the micropower generator system.

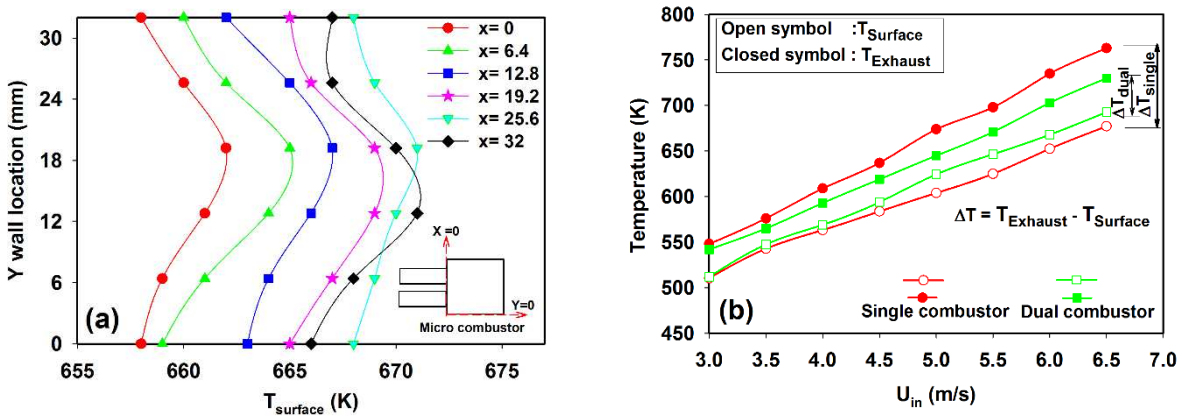

Fig. 7 (a) Wall temperature variation along y-axis at 6 m/s and (b) Variation of average surface and exhaust gas temperature and with total mixture velocity at $\phi = 1.0$.

3.2 Performance of micro power generation system

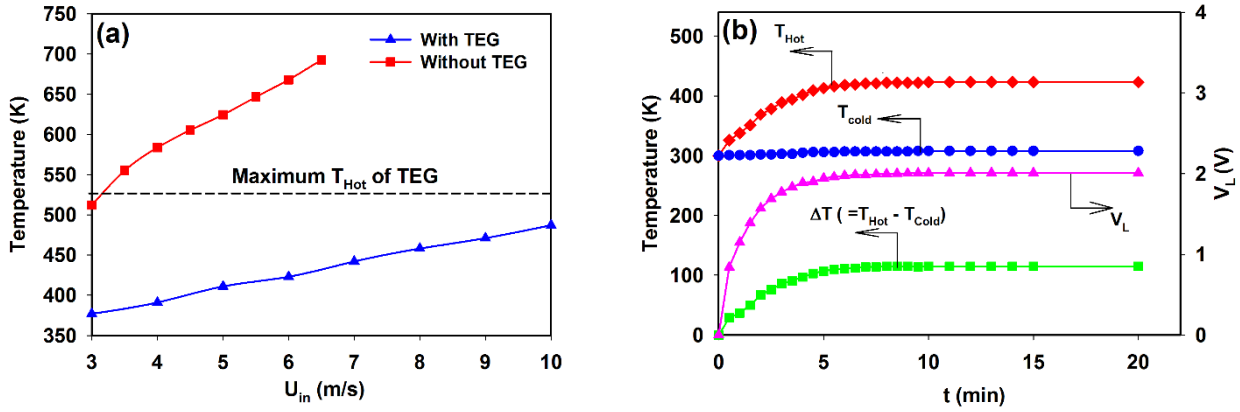

Fig. 8 (a) Variation of temperature with mixture velocity for with and without TEG cases. (b) Temporal variation of temperatures and output voltage for 6.0 m/s at ϕ = 1.0.

A detailed analysis of thermal and performance characteristics of the integrated system has been carried out. The hot side temperature (T_{Hot}) increases with the fuel input for both TEG and no TEG case. Even though the combustor temperature increases beyond 673 K at 6.0 m/s flow velocity, a significant drop in T_{Hot} (~483 K at 10 m/s) is observed, when TEGs are mounted as shown in Fig. 8a. TEG modules absorb significant amount of heat and T_H drops to safe operating limits, which ensures its safe operation within the experiment bounds. Figure 8b shows the temporal variation of T_H, T_C and output voltage (V_L) at a mixture velocity of 6 m/s and ϕ = 1.0. After establishing a stable flame inside the combustor, the ignition port is closed (t = 0 min), and T_{Hot} increases to 423 K within 6 minutes. Then onwards, T_H remains nearly constant until the mixture supply is stopped at t = 25 min, which indicates the steady state of operation of the system. A test study of 1 hour time period has been carried out to understand the working time of the system. The system was able to produce a steady power output after initial 6 mins of starting up time, till the fuel supply ceases. Though T_C also increases after ignition, it does not exceed 308 K during the experiments due to high specific heat of cooling medium. The output voltage of each TEG follows a trend, similar to temperature and reaches its maximum value of 2 V at t = 6 min and remains constant with time. These results indicate that the

system output reaches its maximum value within 6 min and ensure the practicality of the proposed system.

3.2.1 Determination of maximum power output

A 0 – 20 Ω range rheostat is connected in series with the thermoelectric generators to obtain the V-I characteristics for the given conditions and to apply the maximum power point tracking (MPPT) to extract the maximum power from the TEGs. The load resistance (R_L) in the circuit is varied in the step of 0.2 Ω manually and the corresponding voltage is measured using a voltmeter for different fuel inputs. Power output is calculated using $P_{out} = V_L^2/R_L$ formula. This has been also verified by using the formula $P_{out} = V \times I$ for each case. Maximum power from the module is extracted using the technique of maximum power point tracking algorithm and the V-I characteristics are recorded for different electric loads. Figure 9a shows the variation of power with mixture velocity for different load resistances. It can be seen that, the output power peaks towards 4 Ω resistance and decreases on both sides of the load resistance. The maximum power is extracted from the system, when the internal resistance of the module matches with the external load resistance. A similar trend has been observed for all mixture velocities considered in the present work [29, 39, 46]. Figure 9b shows the variation of power output and current with the voltage for a single module case. Maximum power of 2.3 W is obtained with an optimal electric current of 0.9 A. This condition implies the matching of the internal resistance of TEG with the load resistance.

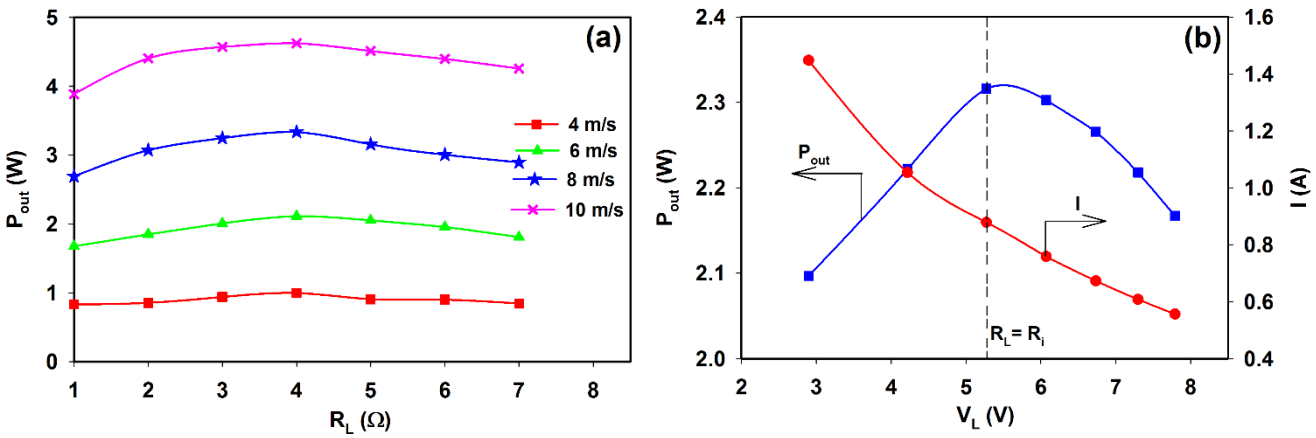

Fig. 9 (a) Variation of power with load resistance for different mixture velocities and (b) Variation of power and current with the voltage at 7 m/s and ϕ = 1.0.

3.2.2 Effect of operating parameters on power generation

Conversion efficiency is defined as the ratio of electrical power output to the chemical energy input. Chemical energy input is calculated from fuel flow rate multiplied with its calorific value. In Fig. 10, several experiments were conducted to understand the effect of coolant flow rate on electrical power output (P_{out}). It is observed that coolant pumping power (P_{aux}) increases from 0.09 W to 0.51 W, when the coolant flow rate increases from 0.5 to 2.0 lpm as shown in Fig. 10. However, no significant variation in power output is observed for flow rates greater than 1.0 lpm due to the higher heating capacity of water. For instance, net power output (P_{out} - P_{aux}) of 2.05 W is achieved at stoichiometric conditions for 6.0 m/s mixture velocity. It is clear from this figure that the pumping power required for driving the coolant is negligible as compared to total power output. Therefore, all the experiments in the present study are conducted at a coolant flow rate of 1.0 lpm.

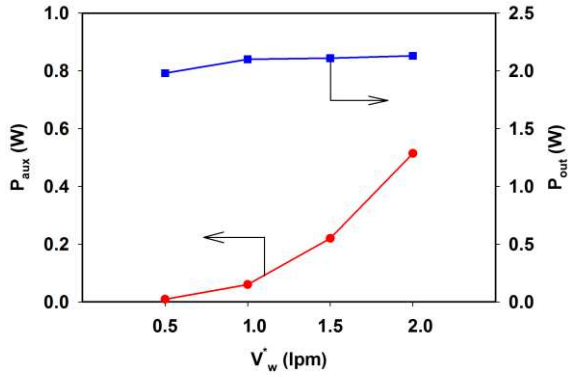

Fig. 10. Variation of auxiliary and electric power output for different coolant flow rate at 6 m/s and ϕ = 1.

Figure 11a shows the variation of output power with mixture velocity for different equivalence ratios. It is observed that nearly equal power is obtained for ϕ = 0.9 and 1.0 mixture conditions. For ϕ = 0.8, a significant reduction in electric power output is observed. This might be due to reduced thermal

input, which results in lower temperature within the combustor and hence lower power output from the modules. Figure 11b shows the variation of overall conversion efficiency with the mixture velocity for different equivalence ratios. Maximum conversion efficiencies of 4.32 %, 4.66 % and 4.19 % are obtained with a corresponding power of 4.62 W, 4.5 W and 3.61 W respectively at ϕ = 1.0, 0.9 and 0.8 with U_{in} = 10 m/s. The obtained power output, power density and conversion efficiencies are significantly higher compared to those reported earlier from such systems.

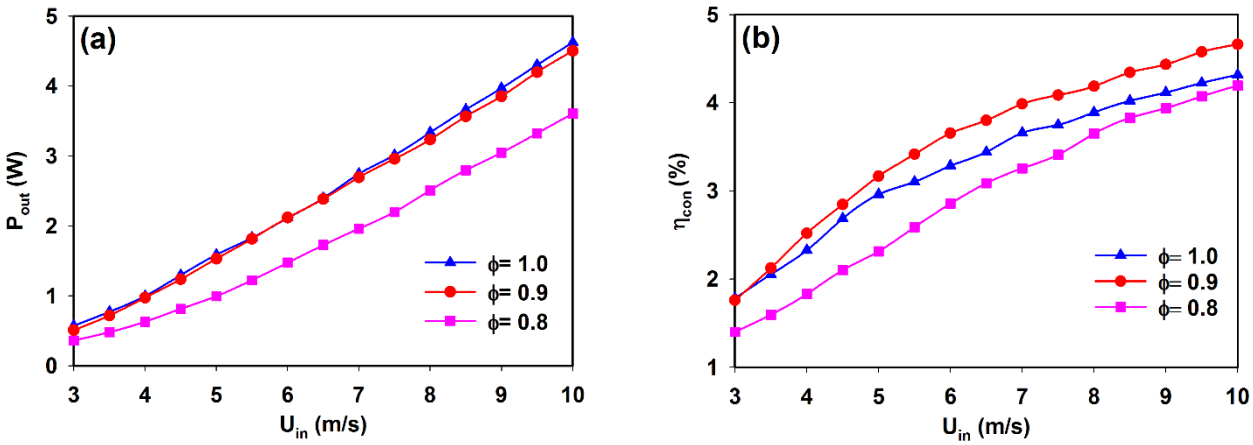

Fig. 11 Variation of (a) Output power (b) Conversion efficiency with total mixture velocity.

3.2.3 Comparison of dual and single microcombustor configurations

A comparison of thermal input and power output as a function of mixture flow rate for single and dual combustor configuration at ϕ = 0.9 is shown in Fig. 12a. The increasing trend of power curve provides an insight into the further increase of mixture flow rate for obtaining higher power outputs. Maximum output power of 3.89 W and 4.6 W is achieved for single and dual combustors respectively for a mixture flow rate of 2.35 g/min (U_{in} = 10 m/s) with an input power of ~ 97 W.

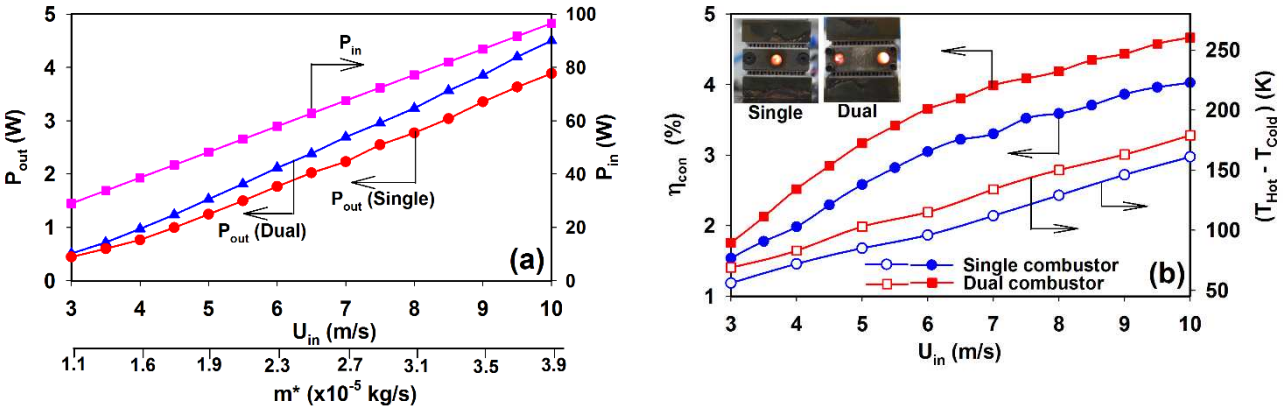

Fig. 12 Comparison of (a) Power output (b) Conversion efficiency and temperature difference for single and dual microcombustors at $\phi = 0.9$.

The conversion efficiency (η_{con}) for both the combustor configurations follows a similar trend as shown in Fig. 12b. The η_{con} is a strong function of combustor wall temperature as electric power output depends on the ΔT, $(T_{Hot} - T_{Cold})$ across the TEG. The distributed temperature profile on the combustor wall and enhanced flame-surface interaction in dual combustor has an increased influence in increasing the wall temperature as discussed earlier. An improvement in the residence time of the reacting mixture due to multiple zones also helps in better heat transfer to the solid wall. This can be clearly attributed from the increase in ΔT $(T_{Hot} - T_{Cold})$ of dual combustor system as shown in Fig. 12b. An increase of 10 – 20 K temperature difference from single to dual combustor results in an increase of ~ 0.2 to 0.6 % in η_{con} for the dual combustor system. Recent numerical studies [37, 38, 47] also predicted similar improvements in thermal characteristics of multichannel microcombustors over a single-channel microcombustor.

A detailed energy balance is obtained for intermediate velocities of 3, 5 and 7 m/s at $\phi = 1.0$. The total heat input to system is chemical energy of the fuel, calculated using fuel flow rate multiplied with its calorific value. The heat loss from TEG to heat sink is determined using Peltier effect, heat conduction and Jules heating effect. The combustor temperature is assumed to be uniform to obtain the convective heat loss through the side surfaces of the heating medium, where TEGs are not mounted. Therefore the total heat lost through the exhaust gas can be expressed as $Q_{exhuast} = Q_{input} - (Q_{sink} + Q_{loss})$. It can be

observed from Table 1 that major part of the heat is lost through exhaust gases ($Q_{exhaust}$), which shows that nearly 60 % of the total heat is rejected to surroundings. Heat rejected through thermoelectric modules to sink (Q_{sink}) is around 20 – 30 % and it increases with an increase in power output from thermoelectric modules. It is interesting to note that, although the heat loss from all parts of the combustor increases with an increase in thermal input, the overall contribution of heat loss in the heat balance decreases (4.4 % to 3.54 %) due to the significant dominance of thermal input over the total heat loss.

Table 1. Energy balance summary for various operating conditions: Q_{in}-Total thermal input, $Q_{exhaust}$ -Heat-loss through exhaust, Q_{loss} – Heat-loss through uncovered sides of system, Q_{sink} – Heat-loss through sink, $P_{electric}$-Electric power generated. Numbers in parentheses show respective percentage.

(W)	U_{in} = 3.0 m/s	U_{in} = 5.0 m/s	U_{in} = 7.0 m/s
Q_{input}	32.14	53.57	75.0
Q_{sink}	9.14 (28.43 %)	15.42 (28.78 %)	22.34 (29.78 %)
Q_{loss}	1.42 (4.4 %)	2.06 (3.85 %)	2.65 (3.54 %)
$Q_{exhaust}$	21.02 (65.39 %)	34.51 (64.41 %)	47.27 (63.03 %)
$P_{electric}$	0.57 (1.78 %)	1.59 (2.96 %)	2.74 (3.66 %)

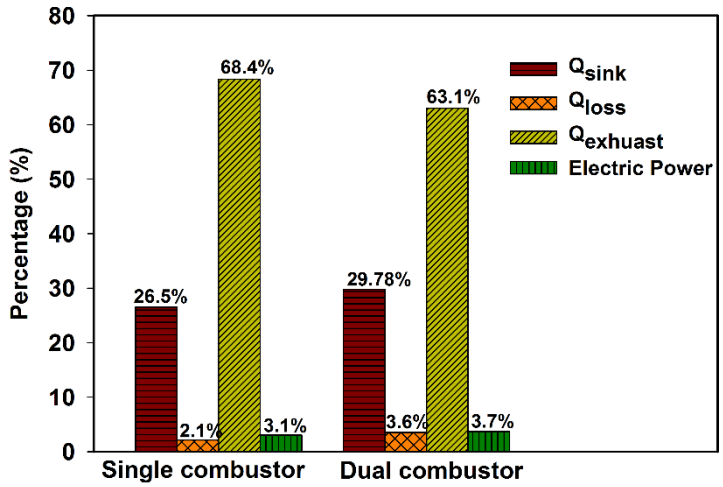

Fig. 13 Comparison of energy balance for single and dual combustor at 7 m/s and ϕ = 1.0.

The heat loss increases (~ 1.5 %) due to increased bare surface area for dual combustor configuration.

A significant improvement in heat transferred to the sink (~ 3.0 %) through solid walls for dual combustor helps to increase power output compared to single combustor (~ 0.6 %) as shown in Fig. 13. The novelty of the present system lies in the design and performance of the dual microcombustor configuration for increased power generation with improved power density of 14 mW/mm^3 as compared to 12 mW/mm^3 for single combustor system. The power density is defined as the ratio of output power to the total volume of the power generator including micro combustor, TEG/TPV and cooling jackets. The overall size of the power generator system is extremely important for portable power applications. Due to high power density, the dual combustor design appears to be a promising alternative for micropower generation and capable of delivering a maximum power of 4.5 W with a conversion efficiency of 4.66 %.

It is interesting to note from Fig. 14 that, though many researchers have came up with various combustion based micro power generators in the past dacades [24, 27, 28, 30, 38], no system in the literature has shown to operate at high overall conversion efficiency(> 4 %) with a high power density (> 0.08 mW/mm^3). There is a significant increase in both the power density and overall conversion efficiency over last two decades. The present micro power generator is an appreciable contribution to the increasing demand of high power density with high conversion efficiency as shown in Fig. 14.

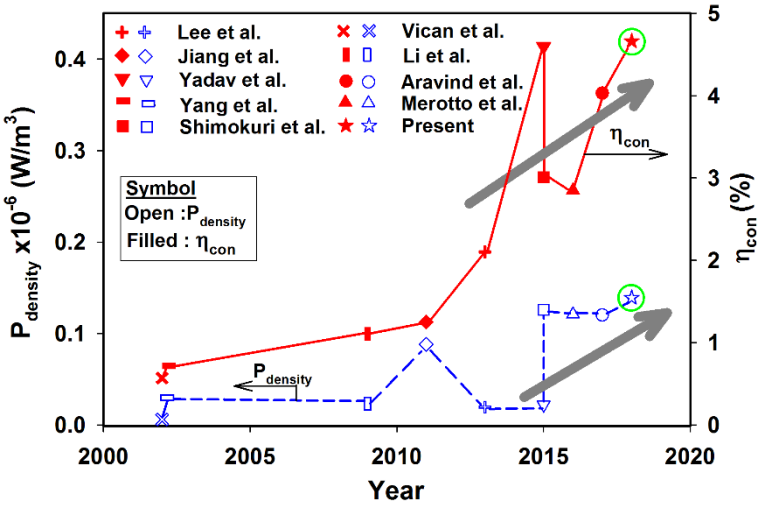

Fig. 14 Performance comparison of combustion based micropower generators.

The present study discusses the performance of an efficient prototype of a micro thermoelectric power generator using premixed LPG-air mixture. The results reveal that, the proposed prototype offers significantly high power density with improved conversion efficiency as compared to the similar power generators reported in the literature. However, it is important to understand the practicality of the system for real life applications. Therefore our research group is currently working on the development of a self-aspirating micro power generator, where air is entrained into the micro combustor from atmosphere through an ejector system using the kinetic energy of the high speed fuel jet. Furthermore, the total size of the system should be reduced further to increase the power density for the next generation stand-alone power generation systems. The present study provides a great insight into the influence of various operating parameters such as inlet velocity and equivalence ratio and the effect of porous media on flame stabilization and power output. This would help in the design and development of a new self-aspirating portable power generator for various real life applications.

4 Conclusions

In the present study, a planar dual microcombustor configuration has been shown to work for power generation with increased power density of 0.14 mW/mm^3 and higher conversion efficiency (4.66 %). Flame stability and thermal characteristics of the proposed dual microcombustor configuration are experimentally investigated. The upper flame stability limits were significantly enhanced with porous media due to preheating of fresh mixture through heat recirculation contribution of porous media. The dual combustor configuration offers superior temperature uniformity and higher surface temperature due to increased flame-surface contact and enhanced heat recirculation. Maximum conversion efficiencies of 4.32 %, 4.66 %, and 4.19 % with a maximum power of 4.62 W, 4.5 W and 3.61 W are achieved for ϕ = 1.0, 0.9 and 0.8 respectively at a mixture velocity of 10 m/s. The major advantages of the present system include (i) Improved thermal and flame stability characteristics of the integrated dual microcombustor (ii) High power density (0.14 mW/mm^3) and high conversion efficiency (4.66 %) of the system, (iv) Easy to fabricate from the application view point (v) Quick startup time for system and non-degradable performance with time.

Acknowledgement

Authors acknowledge the financial support for this work from Science and Engineering Research Board, Department of Science and Technology, Govt. of India wide grant no. SB/S3/COMB-001/2014.

5 References

[1] Fernandez-Pello AC. Micropower generation using combustion: issues and approaches. Proc Combust Inst. 2002;29:883-99.

[2] Walther DC, Ahn J. Advances and challenges in the development of power-generation systems at small scales. Prog Energ Combust Sci. 2011;37:583-610.

[3] Ju Y, Maruta K. Microscale combustion: technology development and fundamental research. Prog Energ Combust Sci. 2011;37:669-715.

[4] Kaisare NS, Vlachos DG. A review on microcombustion: Fundamentals, devices and applications. Prog Energ Combust Sci. 2012;38:321-59.

[5] Cho J-H, Lin CS, Richards CD, Richards RF, Ahn J, Ronney PD. Demonstration of an external combustion micro-heat engine. Proc Combust Inst. 2009;32:3099-105.

[6] Maruta K. Micro and mesoscale combustion. Proc Combust Inst. 2011;33:125-50.

[7] Norton DG, Vlachos DG. Combustion characteristics and flame stability at the microscale: a CFD study of premixed methane/air mixtures. Chem Eng Sci. 2003;58:4871-82.

[8] Kim NI, Aizumi S, Yokomori T, Kato S, Fujimori T, Maruta K. Development and scale effects of small Swiss-roll combustors. Proc Combust Inst. 2007;31:3243-50.

[9] Shirsat V, Gupta A. Performance characteristics of methanol and kerosene fuelled meso-scale heat-recirculating combustors. Appl energy. 2011;88:5069-82.

[10] Chou S, Yang W, Li J, Li Z. Porous media combustion for micro thermophotovoltaic system applications. Appl Energy. 2010;87:2862-7.

[11] Vijayan V, Gupta A. Combustion and heat transfer at meso-scale with thermal recuperation. Appl Energy. 2010;87:2628-39.

[12] Vijayan V, Gupta A. Flame dynamics of a meso-scale heat recirculating combustor. Appl Energy. 2010;87:3718-28.

[13] Shirsat V, Gupta A. A review of progress in heat recirculating meso-scale combustors. Appl Energy. 2011;88:4294-309.

[14] Wierzbicki TA, Lee IC, Gupta AK. Combustion of propane with Pt and Rh catalysts in a meso-scale heat recirculating combustor. Appl Energy. 2014;130:350-6.

[15] Shirsat V, Gupta A. Extinction, discharge, and thrust characteristics of methanol fueled meso-scale thrust chamber. Appl energy. 2013;103:375-92.

[16] Aravind B, Velamati RK, Singh AP, Yoon Y, Minaev S, Kumar S. Investigations on flame dynamics of premixed H 2–air mixtures in microscale tubes. RSC Adv. 2016;6:50358-67.

[17] Wan J, Zhao H. Dynamics of premixed CH4/air flames in a micro combustor with a plate flame holder and preheating channels. Energy. 2017;139:366-79.

[18] Alipoor A, Saidi MH. Numerical study of hydrogen-air combustion characteristics in a novel micro-thermophotovoltaic power generator. Appl Energy. 2017;199:382-99.

[19] Akhtar S, Kurnia JC, Shamim T. A three-dimensional computational model of H2–air premixed combustion in non-circular micro-channels for a thermo-photovoltaic (TPV) application. Appl Energy. 2015;152:47-57.

[20] Akhtar S, Khan MN, Kurnia JC, Shamim T. Investigation of energy conversion and flame stability in a curved micro-combustor for thermo-photovoltaic (TPV) applications. Appl Energy. 2017;192:134-45.

[21] Zuo W, Jiaqiang E, Liu H, Peng Q, Zhao X, Zhang Z. Numerical investigations on an improved micro-cylindrical combustor with rectangular rib for enhancing heat transfer. Appl Energy. 2016;184:77-87.

[22] Waitz IA, Gauba G, Tzeng Y-S. Combustors for micro-gas turbine engines. J Fluids Eng. 1998;120:109-17.

[23] Yang W, Chou S, Shu C, Li Z, Xue H. A prototype microthermophotovoltaic power generator. Appl phy l. 2004;84:3864-6.

[24] Lee S, Um D, Kwon O. Performance of a micro-thermophotovoltaic power system using an ammonia-hydrogen blend-fueled micro-emitter. Int J Hydrogen Energ. 2013;38:9330-42.

[25] Ahn J, Ronney PD, Shao Z, Haile SM. A thermally self-sustaining miniature solid oxide fuel cell. J Fuel Cell Sci Tech. 2009;6:041004.

[26] Yoshida K, Tanaka S, Tomonari S, Satoh D, Esashi M. High-energy density miniature thermoelectric generator using catalytic combustion. J Microelectromech Syst. 2006;15:195-203.

[27] Jiang L, Zhao D, Guo C, Wang X. Experimental study of a plat-flame micro combustor burning DME for thermoelectric power generation. Energ Convers Manag. 2011;52:596-602.

[28] Shimokuri D, Taomoto Y, Matsumoto R. Development of a powerful miniature power system with a meso-scale vortex combustor. Proc Combust Inst. 2017;36:4253-60.

[29] Yadav S, Yamasani P, Kumar S. Experimental studies on a micro power generator using thermo-electric modules mounted on a micro-combustor. Energ Convers Manag. 2015;99:1-7.

[30] Merotto L, Fanciulli C, Dondè R, De Iuliis S. Study of a thermoelectric generator based on a catalytic premixed meso-scale combustor. Appl Energy. 2016;162:346-53.

[31] Hsu C-T, Huang G-Y, Chu H-S, Yu B, Yao D-J. Experiments and simulations on low-temperature waste heat harvesting system by thermoelectric power generators. Appl Energy. 2011;88:1291-7.

[32] Aranguren P, Astrain D, Rodríguez A, Martínez A. Experimental investigation of the applicability of a thermoelectric generator to recover waste heat from a combustion chamber. Appl Energy. 2015;152:121-30.

[33] Chou S, Yang W, Chua K, Li J, Zhang K. Development of micro power generators–a review. Appl Energy. 2011;88:1-16.

[34] Ali H, Yilbas BS, Al-Sharafi A. Innovative design of a thermoelectric generator with extended and segmented pin configurations. Appl Energy. 2017;187:367-79.

[35] He W, Zhang G, Zhang X, Ji J, Li G, Zhao X. Recent development and application of thermoelectric generator and cooler. Appl Energy. 2015;143:1-25.

[36] Fanciulli C, Abedi H, Merotto L, Dondè R, De Iuliis S, Passaretti F. Portable thermoelectric power generation based on catalytic combustor for low power electronic equipment. Appl Energy. 2018;215:300-8.

[37] Su Y, Cheng Q, Song J, Si M. Numerical study on a multiple-channel micro combustor for a micro-thermophotovoltaic system. Energ Conver Manag. 2016;120:197-205.

[38] Zuo W, Jiaqiang E, Peng Q, Zhao X, Zhang Z. Numerical investigations on a comparison between counterflow and coflow double-channel micro combustors for micro-thermophotovoltaic system. Energy. 2017;122:408-19.

[39] Aravind B, Raghuram GK, Kishore VR, Kumar S. Compact design of planar stepped micro combustor for portable thermoelectric power generation. Energ Convers Manag. 2018;156:224-34.

[40] Khandelwal B, Deshpande AA, Kumar S. Experimental studies on flame stabilization in a three step rearward facing configuration based micro channel combustor. Appl Therm Eng. 2013;58:363-8.

[41] Taywade UW, Deshpande AA, Kumar S. Thermal performance of a micro combustor with heat recirculation. Fuel Process Technol. 2013;109:179-88.

[42] Khandelwal B, Sahota GPS, Kumar S. Investigations into the flame stability limits in a backward step micro scale combustor with premixed methane–air mixtures. Journal of Micromechanics and Microengineering. 2010;20:095030.

[43] Kim S, Yokomori T, Kim N, Kumar S, Maruyama S, Maruta K. Flame behavior in heated porous sand bed. Proc Combust Inst. 2007;31:2117-24.

[44] Deshpande AA, Kumar S. On the formation of spinning flames and combustion completeness for premixed fuel–air mixtures in stepped tube microcombustors. Appl Therml Eng. 2013;51:91-101.

[45] Fan A, Minaev S, Kumar S, Liu W, Maruta K. Experimental study on flame pattern formation and combustion completeness in a radial microchannel. Journal of Micromechanics and Microengineering. 2007;17:2398.

[46] Aravind B, Kumar S. Parametric Studies on Thermo-electric Power Generation Using Micro Combustor. Techno-Societal 2016, International Conference on Advanced Technologies for Societal Applications: Springer; 2016. p. 589-97.

[47] Yilmaz H, Cam O, Yilmaz I. Effect of micro combustor geometry on combustion and emission behavior of premixed hydrogen/air flames. Energy. 2017;135:585-97.